

On the equivalence of continuum and lattice models for fluids

Athanassios Z. Panagiotopoulos *

Institute for Physical Science and Technology and Department of Chemical Engineering,

University of Maryland, College Park, MD 20742-2431

January 25, 2000

*Electronic mail: thanos@ipst.umd.edu

Abstract

It was demonstrated that finely discretized lattice models for fluids with particles interacting *via* Lennard-Jones or exponential-6 potentials have essentially identical thermodynamic and structural properties to their continuum counterparts. Grand canonical histogram reweighting Monte Carlo calculations were performed for systems with repulsion exponents between 11 to 22. Critical parameters were determined from mixed-field finite-size scaling methods. Numerical equivalence of lattice and continuous space models, within simulation uncertainties, was observed for lattices with ratio of particle diameter σ to grid spacing of 10. The lattice model calculations were more efficient computationally by factors between 10 and 20. It was also shown that Lennard-Jones and exponential-6 based models with identical critical properties can be constructed by appropriate choice of the repulsion exponent.

1. Introduction

Lattice models are frequently used in simulations and theoretical treatments of fluids, despite the fact that they impose translational order inappropriate for disordered phases. The simplest such model was proposed by Ising in 1925¹. Ising model variations continue to be the subject of active research (e.g.²). Lattice models represent well some aspects of the behavior of real fluids, for example exponents associated with the liquid-vapor critical point. Continuum models are commonly used for quantitative studies of the phase behavior and structural properties of real fluids, because lattice models are not considered suitable for this purpose.

The main advantage of simple lattice models is their computational efficiency, which permits probing of longer time and length scales than is possible for atomistically detailed continuum models. Several previous studies have proposed lattice models that retain some of the realism of continuum models, particularly for modeling macromolecules such as synthetic polymers and proteins. For example, the bond fluctuation model³ maps structural units of a polymer onto monomers occupying multiple lattice sites and allows for fluctuations in the bond length between monomers. A high coordination number diamond lattice has been proposed⁴ and used to study thin films⁵ and demixing in polymer blends⁶. High coordination number lattice models have also been proposed for modeling thermodynamics and kinetic aspects of conformational transitions in proteins⁷.

The present study was motivated by recent work⁹ on a simple cubic lattice version of the restricted primitive model for ionic solutions, in which the ratio of ion diameter to lattice spacing, ζ , was assigned small integer values. Models with $\zeta = 1$ or 2 were found to have phase behavior qualitatively different from the continuum model. However, for $\zeta \geq 3$ the phase behavior was found to be qualitatively identical; the critical point and coexistence curves matched within a few percent. The lattice version of the model was found to be

computationally faster by a factor of 100, because the Ewald sum was replaced with a simple array lookup operation. The main objective of the present study is to investigate whether lattice analogs can be found for common non-polar site-site interaction models. Many atomistically detailed models for real fluids are based on a combination of non-polar with polar or coulombic interactions sites (e.g.¹⁰). The availability of quantitatively accurate lattice models for real fluids would open up possibilities for more efficient simulations of their equilibrium thermodynamic properties.

The outline of this paper is as follows. In Section II we present the key ideas underlying our lattice discretization process and define the intermolecular potentials to be studied. Section III is devoted to a brief description of computational methods used to obtain the liquid-vapor critical parameters and coexistence curves. Section IV presents results for the Lennard-Jones 12-6 potential as a function of the lattice discretization parameter ζ , establishing that the phase envelope, critical properties and structure of the liquid are identical, within simulation uncertainties, for the $\zeta = 10$ lattice model and its continuum counterpart. The lattice model calculations are faster by a factor between 10 and 20 than the corresponding continuum calculations. Section V focuses on studies of the effect of the repulsion exponent α on the critical properties of Lennard-Jones and exponential-6 potentials. It is shown that models with nearly identical critical properties can be constructed by appropriate choice of the repulsion exponent. The paper closes with discussion of the key findings and their possible implications for future work.

2. Models

The key idea underlying this work is illustrated schematically in Fig. 1. Consider a pure fluid consisting of N single-site particles of characteristic diameter σ . Particles interact with any intermolecular potential, $U(\vec{r}^N)$, where \vec{r}^N denotes the positions of the N particles.

The potential may or may not have hard-core interactions and could be non-pair-wise-additive. One can construct a series of lattice models in which allowable positions for the centers of particles are on a grid of characteristic spacing l . While any lattice type could be considered in principle, we use the simple cubic lattice as the basis for all calculations in the present paper. The lattice discretization parameter $\zeta = \sigma/l$ controls how closely the lattice model approaches continuum behavior. For low ζ values, the underlying lattice could have a strong effect on the thermodynamic and structural properties of the system. For example, the pressure equation for a system of non-interacting hard spheres on a lattice of $\zeta = 1$ has the form $P = -ln(1 - \rho)$, rather than the familiar continuum equation of state for hard spheres⁸. However, lattice discretization artifacts must decrease as ζ is increased. Equations of state for hard spheres on lattices with $\lambda > 1$ are not presently available, so it is not possible to provide quantitative estimates of how rapid the convergence to the continuum limit is achieved for this case. Previous work⁹ has established that for particles interacting *via* hard-core plus coulombic potential, $\zeta = 3$ is already sufficiently high so that the system has qualitatively the same phase behavior as the continuum analog.

Two commonly used pair-wise additive potential models appropriate for non-polar systems were studied in this paper. These are the Buckingham exponential-6¹¹ and the Lennard-Jones¹² potential models. The Buckingham exponential-6 potential (abbreviated as "Exp-6" from this point on) is

$$U_{Exp-6}(r) = \epsilon \left[\frac{6}{\alpha - 6} e^{-\alpha(r/r_m - 1)} - \frac{\alpha}{\alpha - 6} \left(\frac{r_m}{r} \right)^6 \right], \quad (1)$$

where r_m is the distance at which the potential has a minimum. The characteristic size parameter σ for this potential is defined as the distance for which $U(r) = 0$ and is obtained numerically. A hard core is introduced at the distance of the (unphysical) maximum of the potential at short distances.

The Lennard-Jones $\alpha - 6$ potential model (abbreviated as "LJ" from this point on) is

$$U_{LJ}(r) = \epsilon \left[\frac{6}{\alpha - 6} \left(\frac{r_m}{r} \right)^\alpha - \frac{\alpha}{\alpha - 6} \left(\frac{r_m}{r} \right)^6 \right]. \quad (2)$$

For the LJ potential, the size parameter σ is given by

$$\sigma = r_m \left(\frac{\alpha}{6} \right)^{-\frac{1}{\alpha-6}} \quad (3)$$

All quantities from this point on are non-dimensionalized using σ and ϵ as characteristic length and energy scales, respectively. For example, T represents the temperature divided by ϵ/k , where k is Boltzmann's constant; P represents the pressure divided by ϵ/σ^3 .

Fig. 2 illustrates the change of shape of the potential functions as the repulsion exponent is increased from $\alpha = 12$ to $\alpha = 22$. Differences between the LJ and Exp-6 functional forms decrease with increasing exponent. For both potential forms, increasing the exponent results not only in steeper repulsion, but also in faster decay of the attractive interactions, a fact that will be used to explain the trends in critical temperature discussed in Section V.

3. Simulation Methods

Histogram-reweighting grand canonical Monte Carlo techniques^{14,15} were used to obtain the phase behavior of the models of interest. The mixed-field finite-size scaling approach of Wilding and Bruce¹⁶⁻¹⁸ was used to estimate critical parameters. Details of the computational approach can be found in previous publications by our group^{19,20} and a recent review article²¹.

A cubic central box of linear dimension L (in units of σ) was used, under periodic boundary conditions. Long-range corrections were applied for all calculations using the method of Theodorou and Suter¹³. The simulation results are therefore for the full (untruncated) potentials. The same method was used for determining the radial distribution function at distances up to $\sqrt{3}L/2$.

A simple cubic grid was used for discretization of the particle positions. The potential

energy of interaction between any two sites on this lattice is translationally invariant. The energy of interaction can be written as

$$U(\vec{r}_{ij}) = U(|x_i - x_j|, |y_i - y_j|, |z_i - z_j|), \quad (4)$$

where x , y and z are integers between 0 and $L \times \zeta - 1$. $L \times \zeta$ must be an integer, even though L and ζ can take any real value individually, in order to allow periodic boundary conditions on the simple cubic lattice. Eq. 4 suggests that the potential of interaction can be calculated *once* at the beginning of a simulation and stored in an array of length $(L \times \zeta)^3$. For the potentials studied in the present paper, this method was found to be more efficient by a factor between 10 to 20 relative to calculations in continuous space. The speedup ratio may be sensitive to coding details, machine architecture and compilation parameters. In our study, no special efforts beyond automatic compiler optimization were made for accelerating the lattice or continuum computations. The lower speedup ratio applies to potentials (such as LJ with $\alpha = 12$) that do not require exponentiation or raising of a real number to a non-integer power. This surprisingly high acceleration of the lattice calculations relative to continuum results from elimination of the minimum distance image and potential function evaluation for every interacting pair. While this improvement in computational efficiency is less spectacular than that observed in⁹ for coulombic interactions, it is still quite significant.

Runs of 30×10^6 to 300×10^6 Monte Carlo steps were performed near critical points, with longer runs utilized for bigger system sizes. Much shorter runs of $3-10 \times 10^6$ Monte Carlo steps were performed away from critical points to obtain the phase diagrams and evaluate the pressure by calculating the partition function at low densities²⁰. A move mix of 70% attempted insertions/deletions and 30% attempted particle displacements was used. Statistical uncertainties were obtained by performing four duplicate sets of runs at identical conditions with different seeds for the random number generator. The "ran2" routine of reference²², which has a period of 2.3×10^{18} and no low-order serial correlations, was used.

A typical run of 50×10^6 Monte Carlo steps in a $7 \times 7 \times 7$ box at the critical density took 22 minutes on a Pentium III 450 MHz workstation; the short (3×10^6 steps) run for the saturated liquid which produced the lattice radial distribution function data of the following section took 3.4 minutes.

4. LJ 12-6 model on a lattice

The first objective of this work was to establish the equivalence of lattice and continuum versions of the potentials of interest. For this purpose, a detailed study of the LJ potential with $\alpha = 12$ was performed. Fig. 3 shows the phase behavior of this model as a function of the lattice discretization parameter ζ . The phase diagram is displaced to higher temperatures and densities for low values of ζ , but the results converge quickly with increasing values of ζ to the continuum limit. Data for $\zeta = 10$ are indistinguishable, within statistical uncertainties, from continuum results of reference²⁰ and from results using the equation-of-state of Johnson *et al.*²³, shown as the continuous line in Fig. 3. The Johnson *et al.* equation-of-state overpredicts the critical point obtained from more recent simulations²⁰, so we chose not to reproduce its predicted phase envelope in the immediate vicinity of the critical point.

Having established that the $\zeta = 10$ lattice model is indistinguishable from the continuum model with respect to the liquid-vapor phase envelope, a detailed study of the finite-size dependence of the critical parameters was performed. Table 1 shows the dependence with linear system size L of the apparent critical temperature T_c , chemical potential μ_c , density ρ_c and pressure P . The apparent critical parameters were obtained by matching the scaled distribution of the order parameter to the universal Ising form.

Fig. 4 shows the dependence of the apparent critical temperature to the scaled linear length, $L^{-(\theta+1)/\nu}$, where the values of the critical exponents $\theta = 0.54$ and $\nu = 0.629$ are appropriate for the three-dimensional Ising universality class. Comparable values for the

critical parameters as functions of system size for the full (untruncated) LJ 12-6 potential are available from²⁰. The extrapolated infinite-system critical parameters were reported in²⁰ as $T_c = 1.3120 \pm 0.0007$, $\mu_c = -3.562 \pm 0.001$, $\rho_c = 0.316 \pm 0.001$ and $P_c = 0.1279 \pm 0.0006$. There is good agreement between the lattice and continuum results for all lengths, within simulation uncertainties. The $\zeta = 10$ lattice and continuum models have identical dependence of the apparent critical properties on system size. There is nothing special about the LJ 12-6 potential relative to the other potentials of interest in the present study, so this equivalence is expected to hold for the other models studied.

One may argue that lattice models are inherently different from continuum models with respect to the short-distance structure of disordered fluid phases. Fig. 5 compares the $\zeta = 10$ lattice model results to continuum values at conditions corresponding to the saturated liquid at $T = 1.06$. Both lattice and off-lattice calculations were performed on $L = 7$ systems for 3×10^6 Monte Carlo steps, with the radial distribution function sampled every 25,000 steps. There is no difference between the lattice and continuum radial distribution function, within simulation statistical uncertainties. For $\zeta = 10$, the lattice model has a sufficiently large number of possible positions even at short distances to make the radial distribution function behave in a quasi-continuous fashion. For example, there are 318 distinct lattice positions at distances between σ and $1.02 \times \sigma$ from any given site.

5. LJ and Exp-6 models with variable exponent

In the previous section, it was established that high- ζ lattice models and continuum models are quantitatively equivalent with respect to thermodynamic and structural properties of the fluid phases. The effect of the repulsion exponent α on the vapor-liquid critical point for the LJ and Exp-6 lattice models was subsequently investigated. A previous study of coexistence properties of Exp-6 fluids with variable repulsion exponent α has appeared²⁴,

but no comparable study for LJ potentials could be located.

Table 2 presents our results for the critical parameters of LJ and Exp-6 lattice models with $\zeta = 10$ as a function of the exponent α . A linear system size of $L=7$ was used for these calculations. Based on the results of the previous section, we expect the lattice model results to be identical to corresponding continuum models of the same linear size for this (high) value of ζ . For the Exp-6 fluids of $\alpha = 12$ to 18, a comparison of the present data with those in Table I of²⁴ indicates that the critical temperatures reported here are systematically higher by an average of 0.7%. Results of²⁴ were obtained with a system size of $L=5$, while the present results are for $L=7$. The difference (from Table 1) between the apparent T_c for these two system sizes for the $\alpha=12$ LJ lattice models is 0.8%. Similar trends are observed for the critical densities and pressures. We conclude that the present results are in good agreement with those of the previous study.

The results of Table 2 are expected to differ systematically from the corresponding infinite-system values because of finite-size effects. Based on the observed dependence of the apparent critical parameters on system size from Table 1, the true (infinite system) critical temperature is expected to be approximately 1% higher and the critical pressure 4% higher relative to $L=7$. Finite-size effects for the critical density are expected to be comparable to the statistical uncertainties of approximately 1%.

As discussed in Section II, increasing the exponent α results in a shift of the attractive part of the potential to lower separations. It is, therefore, reasonable to expect that the critical temperature and pressure of higher- α models will be lower, while the critical density will be higher. These are indeed the trends observed in Table 2 for both LJ and Exp-6 models.

An interesting question is related to the possible equivalence of LJ and Exp-6 potentials. Some recent models for hydrocarbons²⁵ and water¹⁰ utilize the Exp-6 functional form to

describe non-polar interactions. The large majority of realistic potential models have been based on the LJ functional form. Since it is not clear how one would obtain unlike-pair interactions for sites described by potentials of different functional form, it is desirable to develop a correspondence between them so that parameters can be transferred from LJ to Exp-6 based models and *vice versa*. The critical temperatures of the LJ and Exp-6 models are compared in Fig. 6. The critical temperatures of Exp-6 models are higher than for LJ models of the same value of α , consistent with the faster decay of the LJ functional form seen in Fig. 2. This difference diminishes for higher values of α . Table 2 can be used to obtain approximately equivalent Exp-6 and LJ models. For example, by simple linear interpolation, we find that the LJ model with $\alpha = 15.1$ has the same critical temperature as the Exp-6 model with $\alpha = 16$. The critical density and pressure for the LJ $\alpha = 15.1$ model are estimated (again from linear interpolation) as $\rho_c = 0.323 \pm 0.003$ and $P_c = 0.111 \pm 0.001$, in agreement with the actual parameters for the Exp-6 model with $\alpha = 16$.

6. Discussion

The main conclusion of the present study is that finely discretized lattice models are essentially equivalent to corresponding continuum models. This was demonstrated by studies of the liquid-vapor phase coexistence curve, the dependence of critical parameters on system size and the structure of the liquid measured by the radial distribution function. Monte Carlo calculations for lattice models are, however, significantly faster than their continuum counterparts. The relative speed advantage for non-polar interactions observed in the present study was a factor of 10-20, while an earlier study⁹ for hard-sphere + coulombic interactions obtained a speedup of 100 for Ewald-sum based calculations. Thus, we propose that high- ζ lattice models are suitable for fast simulations of equilibrium properties of atomistically detailed site-site models. For prediction of transport properties, one would then

perform conventional molecular dynamics simulations for the equivalent continuum models. The advantage of the combined approach is that optimization of intermolecular potential parameters to the equilibrium properties would be much faster. It may be also possible in the future to develop molecular dynamics algorithms suitable for finely-discretized lattices.

All calculations in the present work were performed in the grand canonical ensemble. Traditional ($\zeta=1$) lattice models require special techniques to allow calculations in the constant-pressure²⁶ and the Gibbs ensemble²⁷. The reason for this is the large relative change in volume resulting from deletion or addition of a complete layer for low- ζ models, which in turns results in extremely low acceptance ratios of the corresponding attempted moves. However, for the finely discretized models proposed here, the relative change in volume associated with addition or deletion of a complete layer becomes smaller as ζ is increased, so it is expected that calculations in Monte Carlo ensembles that require volume changes should be feasible.

The critical parameters of LJ and Exp-6 models with variable repulsion exponent α were obtained in the present study for a single system size, to within statistical uncertainties of approximately $\pm 0.1\%$ for the temperature and $\pm 1\%$ for the density and pressure. The critical temperature and pressure decrease with increasing α and the critical density increases. Based on our results, LJ and Exp-6 models can be obtained with nearly identical critical parameters. It remains to be seen whether the LJ and Exp-6 model equivalence is also true for multi-site models that include other types of interactions, for example fixed-point charge models for water¹⁰.

7. Acknowledgements

Funding for this research was provided by the Department of Energy, Office of Basic Energy Sciences (DE-FG02-98ER14858). Additional support was provided by the Petroleum

Research Fund administered by the American Chemical Society (grant 34164AC9). I am grateful to Prof. Michael Fisher, Prof. Sanat Kumar and Dr. Jeffrey Errington for helpful discussions and comments on the manuscript.

REFERENCES

1. E. Ising, *Z. Phys.* **31**, 253 (1925).
2. E. Luijten and K. Binder, *Phys. Rev. E* **58**, R4060 (1998).
3. I. Carmesin and K. Kremer, *Macromolecules* **21**, 2819 (1988); H. P. Deutsch and K. Binder, *J. Chem. Phys.* **94**, 2294 (1991).
4. R. F. Rapold and W. L. Mattice, *J. Chem. Soc. Faraday Trans.* **91**, 2435 (1995).
5. P. Doruker and W. L. Mattice, *Macromolecules* **31**, 1418 (1998); *Macromol. Theor. Simul.* **8** 463 (1999).
6. T. Haliloglu and W. L. Mattice, *J. Chem. Phys.* **111**, 4327 (1999).
7. A. Kolinski, W. Galazka and J. Skolnick, *J. Chem. Phys.* **108**, 2608 (1998).
8. N. F. Carnahan and K. E. Starling, *J. Chem. Phys.* **51** 635 (1969).
9. A. Z. Panagiotopoulos and S. K. Kumar, *Phys. Rev. Lett.* **83** 2981 (1999).
10. J. R. Errington and A. Z. Panagiotopoulos, *J. Phys. Chem. B* **102**, 7470 (1998).
11. R. A. Buckingham, *Proc. Roy. Soc.* **A168**, 264 and 378 (1938).
12. J. E. Lennard-Jones, *Proc. Roy. Soc.* **A106**, 441 and 463 (1924).
13. D. N. Theodorou and U.W. Suter, *J. Chem. Phys.* **82**, 955 (1985).
14. A. M. Ferrenberg and R. H. Swendsen, *Phys. Rev. Lett.* **61**, 2635 (1988).
15. A. M. Ferrenberg and R. H. Swendsen, *Phys. Rev. Lett.* **63**, 1195 (1988).
16. N. B. Wilding and A. D. Bruce, *J. Phys. Condens. Matter* **4**, 3087 (1992).
17. A. D. Bruce and N. B. Wilding, *Phys. Rev. Lett.* **68**, 193 (1992).

18. N. B. Wilding, *Phys. Rev. E*, **52**, 602 (1995).
19. A. Z. Panagiotopoulos, V. Wong and M. A. Floriano, *Macromolecules* **31**, 912 (1998).
20. J. J. Potoff and A. Z. Panagiotopoulos, *J. Chem. Phys.* **109** 10914 (1998).
21. A. Z. Panagiotopoulos, *J. Phys. Condens. Matter* **12**, R25 (2000).
22. W. H. Press, S. A. Teukolsky, W. T. Vetterling and B. P. Flannery, *Numerical Recipes in FORTRAN*, 2nd Ed., Cambridge U. Press: Cambridge, UK (1992).
23. J. K. Johnson, J. A. Zollweg and K. E. Gubbins, *Molec. Phys.* **78**, 591 (1993).
24. J. R. Errington and A. Z. Panagiotopoulos, *J. Chem. Phys.* **109**, 1093 (1998).
25. J. R. Errington and A. Z. Panagiotopoulos, *J. Phys. Chem. B* **103**, 6314 (1999).
26. A. D. Mackie, A. Z. Panagiotopoulos, D. Frenkel and S. K. Kumar, *Europhys. Lett.* **27**, 549 (1994).
27. A. D. Mackie, A. Z. Panagiotopoulos and S. K. Kumar, *J. Chem. Phys.* **102**, 1014 (1995).

TABLES

Table 1. Apparent critical parameters for LJ lattice models with $\alpha = 12$, $\zeta = 10$ as a function of the linear system size, L . Numbers in parentheses indicate statistical uncertainties in units of the last digit of the corresponding value.

L	T_c	μ_c	ρ_c	P_c
5	1.289(1)	-3.583(1)	0.314(1)	0.122(1)
7	1.299(2)	-3.575(2)	0.316(3)	0.123(1)
9	1.303(2)	-3.571(2)	0.317(2)	0.124(1)
12	1.308(1)	-3.568(1)	0.317(3)	0.126(1)
15	1.311(1)	-3.567(1)	0.317(2)	0.127(1)

Table 2. Apparent critical parameters for LJ and Exp-6 lattice models with $\zeta = 10$, $L = 7$, as a function of the exponent α . Numbers in parentheses indicate statistical uncertainties in units of the last digit of the corresponding value.

α	T_c	μ_c	ρ_c	P_c
LJ				
11	1.368(2)	-3.774(2)	0.315(2)	0.129(1)
12	1.299(2)	-3.575(2)	0.316(3)	0.123(1)
14	1.196(2)	-3.280(1)	0.320(3)	0.114(1)
16	1.125(2)	-3.069(2)	0.326(2)	0.109(1)
18	1.071(2)	-2.911(1)	0.330(3)	0.106(1)
20	1.028(2)	-2.790(2)	0.333(3)	0.101(1)
22	0.993(1)	-2.692(1)	0.336(2)	0.099(1)
Exp-6				
12	1.404(1)	-3.805(2)	0.314(3)	0.132(1)
14	1.253(2)	-3.521(3)	0.321(3)	0.120(1)
16	1.157(1)	-3.331(1)	0.326(2)	0.112(1)
18	1.088(2)	-3.194(1)	0.327(2)	0.105(1)
20	1.039(1)	-3.086(2)	0.329(1)	0.102(1)
22	1.000(1)	-2.997(1)	0.332(3)	0.098(1)

FIGURES

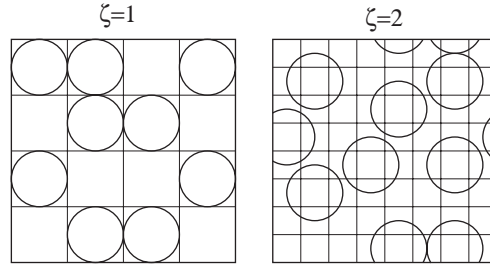


Fig. 1. Schematic illustration of the lattice discretization process for $\zeta = 1$ and 2. A two-dimensional system is shown for simplicity, even though all calculations were performed for three-dimensional systems. Periodic boundary conditions are implied, so that particles near the box edges appear split.

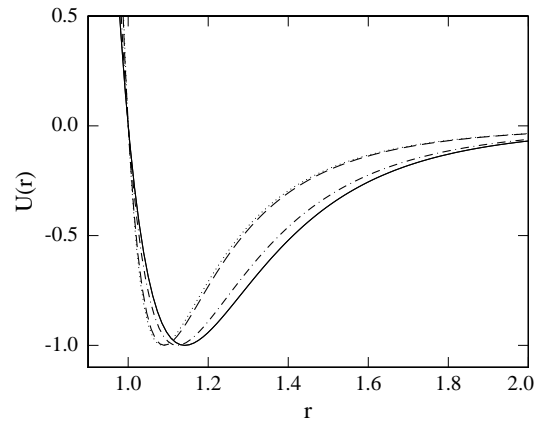


Fig. 2. Potential energy, $U(r)$, versus distance r for the following models: $\alpha = 12$: Exp-6 (solid line) and LJ (dash-dotted line); $\alpha = 22$: Exp-6 (dashed line) and LJ (dotted line).

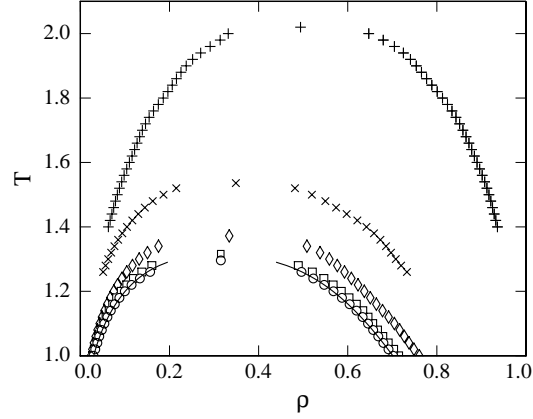


Fig. 3. Phase diagrams for LJ lattice models with $\alpha = 12$. Points are for $\zeta = 1$ (crosses), 2 (\times 's), 3 (diamonds), 5 (squares) and 10 (circles). System size was $L = 10$ for the first three values of ζ and $L = 8$ and 7 , respectively, for $\alpha = 5$ and 10 . Line is for the continuum model, from the equation-of-state of Johnson *et al.*²³. Statistical uncertainties are smaller than the symbol size.

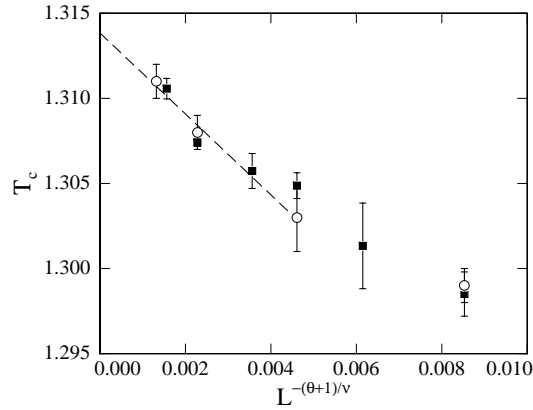


Fig. 4. Critical temperature, T_c , as a function of scaled system size, $L^{-(\theta+1)/\nu}$, for LJ models with $\alpha = 12$. Open circles are for lattice models with $\zeta = 10$ and filled squares are continuum results from²⁰. The dashed line represents a linear least-squares fit to the three highest system sizes of the lattice models.

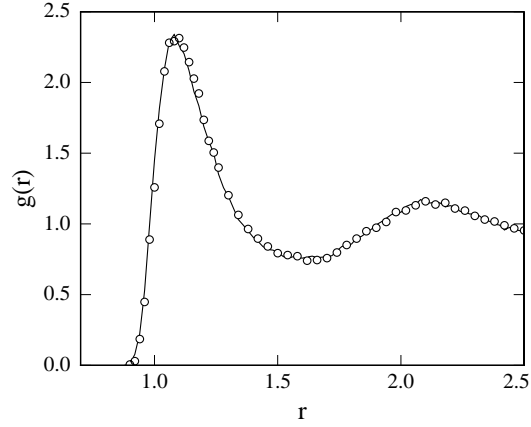


Fig. 5. Radial distribution function, $g(r)$, versus distance r for LJ lattice (points) and continuum models (line). For both models, $\alpha = 12$, $L = 7$, $T = 1.06$ and $\mu = -3.702$, corresponding to the saturated liquid phase.

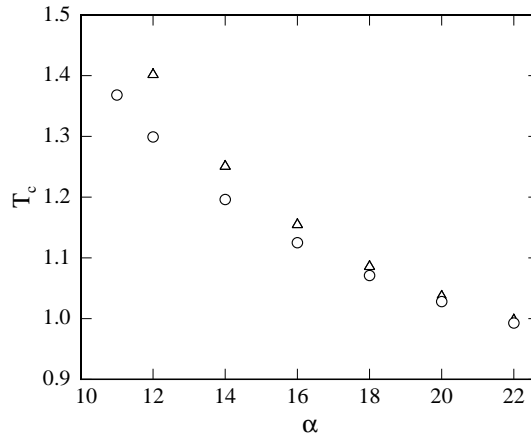


Fig. 6. Critical temperature, T_c , as a function of exponent α for LJ (circles) and Exp-6 (triangles) lattice models with $\zeta = 10$ and $L = 7$. Statistical uncertainties are smaller than the symbol size.